THE JOURNAL OF PHYSICAL CHEMISTRY C

Article

pubs.acs.org/JPCC

Assessing the Potential of Peropyrene as a Singlet Fission Material: Photophysical Properties in Solution and the Solid State

Valerie M. Nichols,[†] Marco T. Rodriguez,[‡] Geoffrey B. Piland,[†] Fook Tham,[†] Vladimir N. Nesterov,[‡] W. Justin Youngblood,[‡] and Christopher J. Bardeen*,[†]

[†]Department of Chemistry, University of California, Riverside, Riverside, California 92521, United States

[‡]Department of Chemistry, University of North Texas, Denton, Texas 76203, United States

Supporting Information

ABSTRACT: The photophysical behavior of the polycyclic aromatic hydrocarbon peropyrene is studied both in dilute solution and in the solid state, with the goal of evaluating this molecule as a singlet fission (SF) material. In solution, the fluorescence quantum yield is consistently in the range 0.90−0.95, while the fluorescence lifetime changes from 3.2 to 5.5 ns. Analysis of the solvent dependence of the radiative rate provides evidence that the bright ^1B_u singlet state mixes with a second, optically dark state. The presence of a dark state slightly above the ^1B_u state in energy is confirmed using two-photon fluorescence excitation spectroscopy. The crystal structure of solid peropyrene consists of a herringbone arrangement of π-stacked molecular pairs, similar to the α-polymorph of perylene. There are two emitting species, centered at approximately 550 and 650 nm, both of which are formed within the 15 ps time resolution of the experiment, and which relax independently via biexponential decays. We find no evidence for rapid SF in the peropyrene crystals, most likely due to the large shift of the singlet state to lower energy where it no longer fulfills the energy condition for SF. These results demonstrate how both energetics and crystal packing influence the ability of a molecule to function as a SF material.

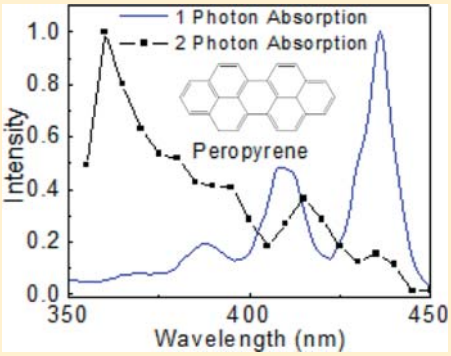

INTRODUCTION

Polycyclic aromatic hydrocarbons (PAHs) have received increased interest from the chemical research community for a variety of reasons. Although early research mostly focused on their role as industrial pollutants and human carcinogens, there is now growing interest in this class of molecules for applications in electronic devices such as photovoltaic solar cells and thin-film transistors. Graphene is perhaps the most dramatic example of how the unique electronic properties of the PAH family can give rise to a variety of potential applications. But smaller members of the PAH family can also have interesting and potentially useful properties.[1] For example, polyacenes like tetracene and pentacene have large electron exchange interactions that lead to large energy gaps between their triplet (T_1) and singlet (S_1) excited states.[2] When $2E(T_1) \leq E(S_1)$, the generation of two triplet states from one singlet becomes energetically possible. This singlet fission (SF) reaction[3,4] is spin-allowed and, if the two triplets can be efficiently ionized,[5−7] it provides a way for a single high-energy photon to generate two electron−hole pairs. If a SF material is paired with a second, low bandgap semiconductor, then the more efficient utilization of the high-energy portion of the solar spectrum could lead to photovoltaic efficiencies ∼30% higher than those predicted by the Schockley-Queisser limit.[8]

The potential utility of SF for solar cell applications has led to a resurgence of interest in this phenomenon, first identified in 1965 in crystalline anthracene.[9] Recent time-resolved studies have concentrated on the polyacenes tetracene[10−13] and pentacene,[14−20] although other classes of conjugated molecules have the potential to exhibit SF, with efficient SF in carotenoids[21] and isobenzofurans[22] having been demonstrated recently. The rylene family has also attracted interest as potential SF materials, since perylene diimides fulfill the energetic criterion $2E(T_1) \approx E(S_1)$.[23] In fact, SF has been observed in crystalline perylene (PER) through the observation of magnetic field effects in its fluorescence signal.[24−26] However, because $2E(T_1) > E(S_1)$ in PER, SF requires excess energy, similar to the case of anthracene. In this case, SF must compete with intramolecular relaxation to the lowest vibrational level and is not expected to be very efficient. Extending the conjugation of the PER ring should lower its triplet energy, with the simplest strategy being a symmetric extension of the ring system to make peropyrene (PP), whose structure is shown in Figure 1. Solution phase measurements on PP indicate that its triplet state is almost exactly half the energy of its singlet state,[27] with $E(T_1)$ = 11 000 cm^{-1} and $E(S_1)$ = 22 500 cm^{-1}, making this molecule a good candidate for SF. Furthermore, the well-known photostability of the perylene family, along with their high absorption cross section, could make PP a more practical alternative to polyacenes like

Received: May 24, 2013
Revised: July 12, 2013
Published: July 17, 2013

   dx.doi.org/10.1021/jp4051116 | J. Phys. Chem. C 2013, 117, 16802−16810

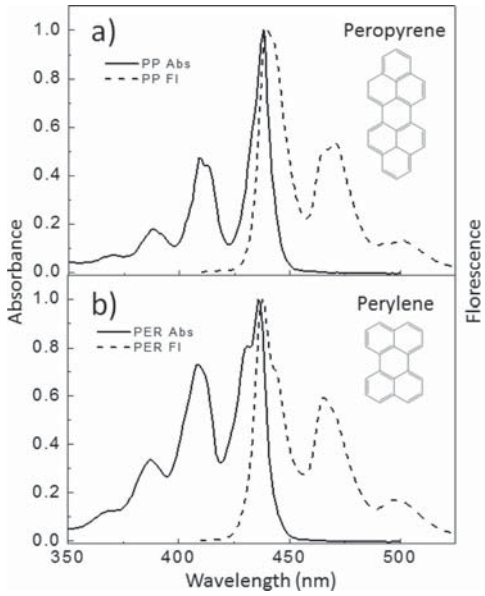

Figure 1. Normalized steady state absorption (solid) and the steady state fluorescence (dashed) of (a) monomeric peropyrene (PP) and (b) monomeric perylene (PER) in cyclohexane.

tetracene for photovoltaic applications. In this paper, we study the photophysics of PP both in dilute solution and in the solid-state, with the goal of evaluating it as a potential SF material. Our analysis of the spectroscopic properties of molecules in dilute solution provide evidence that the low-lying triplet states of this molecule affect the properties of the singlet state through mixing of an optically dark state with the bright ^1B_u state. This mixing, previously observed only in polyenes, leads to a dramatic dependence of the radiative rate on solvent polarizability. We report the crystal structure of solid peropyrene for the first time, finding that its packing is very similar to that of the α -polymorph of PER. The face-to-face packing leads to large changes in the singlet fluorescence. We find no evidence for rapid SF in the PP crystals, most likely due to the large shift of the singlet state to lower energy in the crystal so that $E(S_1) < 2E(T_1)$. Our results demonstrate how both energetics and crystal packing influence the ability of a molecule to function as a SF material, and we suggest ways to improve the ability of PP to function as a SF material.

EXPERIMENTAL SECTION

Peropyrene (PP) was synthesized following a reported procedure.[28] $TiCl_4$ (160 μL, 1.44 mmol) was injected dropwise to a stirring suspension of $LiAlH_4$ (58 mg, 1.4 mmol) in dry THF (10 mL) at 0 °C under argon. The mixture was allowed to warm slowly to room temperature and then was heated to reflux for 90 min. Phenalenone (0.20 g, 1.1 mmol) in THF (5 mL) was added to the mixture. Stirring and heating continued for three days, and additional THF was added as necessary. The reaction was then allowed to cool, and the remaining $LiAlH_4$ was quenched with isopropanol/hexanes (1:1) at 0 °C. The emulsion was concentrated in vacuo and the solid was extracted with toluene. The product was purified by adsorption chromatography (SiO_2, hexanes, toluene 3:1) followed by size exclusion chromatography (Bio-Beads SX-3, toluene) to give the product as a yellow solid (11 mg, 5%). Recrystallization from hot *o*-xylene under argon gave yellow plates. The NMR data were consistent with previous reports.[28,29] ^{1}H NMR (500 MHz, C_6D_6) δ 7.92 (t, J = 7.6 Hz, 2H), 8.15 (d, J = 7.6 Hz, 4H), 8.16 (d, J = 9.2 Hz, 4H), 8.99 (d, J = 9.2 Hz, 4H); λ_{Abs} = 392, 415, 442 nm. The complete NMR and UV−vis spectra are given in the Supporting Information.

Perylene (PER) was purchased from Sigma Aldrich and used as received. Monomer samples of PP and PER were made by dissolving the solids in solutions of cyclohexane, acetonitrile, toluene, tetrahydrofuran, dichloromethane, dimethyl formamide, chlorobenzene, ethanol, and chloroform at 10^{-5} M concentrations. All solvents were purchased from Sigma Aldrich (HPLC grade, >99.9%) and were used as received.

Absorption spectra of liquid samples were taken in a 1 cm quartz cuvette in a Cary 50 spectrometer. Steady state fluorescence spectra were measured under vacuum in a Janis ST100 cryostat with a Fluorolog 3 spectrofluorimeter with 400 nm excitation and front face detection. Fluorescence quantum yield experiments were performed using liquid samples with optical densities ranging from 0.02 to 0.1 to avoid self-absorption effects. The fluorescence data were taken using 385 nm excitation and PER in cyclohexane as the reference (quantum yield = 0.94[30,31]). To avoid quenching by O_2, samples were sealed in a 1 cm quartz cuvette with an overpressure of argon after being bubbled under argon for 15 min.

Fluorescence lifetime data were taken using front face detection with a Hamamatsu C4334 streakscope picosecond streak camera with a time resolution of 15 ps. The 400 nm excitation pulse was generated by frequency doubling the 800 nm pulse with a pulse width of 150 fs from a 40 kHz Spectra-Physics Spitfire Ti:sapphire regenerative amplifier. Scattered pump light was removed by placing a 450 nm long wave pass filter and 420 nm color filter on the input lens before the streak camera. The fluorescence was detected at 54.7° relative to the pump to eliminate rotational diffusion effects. The pulse fluences were kept below 1.2 μJ/cm^2, and measurements of the fluorescence decay at different laser intensities yielded similar decays, indicating that exciton−exciton annihilation did not influence the results.

Two-photon excitation spectra were taken using a Mai Tai wide-band, mode-locked Ti:sapphire laser scanning in 10 nm increments from 710 to 920 nm. Samples were held in a 1 cm quartz cuvette and fluorescence was collected at 90° using a photomultiplier tube. The fluorescence intensity was recorded using a lock-in amplifier. Multiple powers were tested to confirm that the fluorescence intensity was proportional to the square of the laser power, characteristic of a two-photon absorption process.

Single-crystal X-ray diffraction data were collected on a Bruker APEX2 platform CCD X-ray diffractometer system (Mo-radiation, λ = 0.71073 Å, 50 kV/40 mA power) at 296. The frames were integrated using the Bruker SAINT software package and a narrow-frame integration algorithm. Absorption corrections were applied to the raw intensity data using the SADABS program. The Bruker SHELXTL software package was used for phase determination and structure refinement.

All calculations were done with the Gaussian 09 quantum chemistry package.[32] The computational method used for this work was TD-B3LYP using the 6-31 G* double-ζ basis set.[33,34] Geometries converged with a force threshold of 0.00045 au and a displacement threshold of 0.001800 au. Ground state geometries were obtained using B3LYP/6-31 G* with no symmetry restrictions and these geometries were subsequently

used for calculating the vertical excitations of PP. Energy minima were confirmed by ensuring the Hessian contained no imaginary values.

RESULTS AND DISCUSSION

Peropyrene (PP) was synthesized using a reductive coupling reaction mediated by low-valent titanium. We found that the yield of this reaction was considerably lower than the 40% reported in ref 28. The presence of a large number of other unknown products of varying polarity required both adsorption and gel permeation chromatography to isolate peropyrene from the reaction mixture. The other route to PP in the literature involves high temperature heating of the starting materials in the presence of zinc dust[35,36] that also produces PP in a complex product mixture. Although the zinc dust preparation allows for convenient scale-up of the PP-forming reaction, the poor solubility of the desired product greatly hinders the separation of large scale mixtures.

PP is a highly absorbing molecule ($\varepsilon = 1.1 \times 10^5\ M^{-1}\ cm^{-1}$ at its peak absorption[27]) that is very photostable. Solutions of the molecule left out in air at room temperature under room lights showed no decrease in absorption after 1 week. PP is also highly fluorescent, with a quantum yield greater than 90% in most solvents. The molecule is very similar to perylene (PER) in terms of its spectral properties and photostability, and despite its larger π-electron conjugation extent, its absorption and emission are only shifted by ~5 nm to the red as compared to PER. Figure 1a shows the absorption and fluorescence spectra of PP in cyclohexane, which can be compared to those of PER in Figure 1b. A plot of the Stokes shift versus the solvent orientation polarizability (Supporting Information, Figure S3) had a negligible slope, reflecting the fact that the absorption and fluorescence shift by similar amounts in different solvents. The lack of a Stokes shift dependence on solvent polarity indicates that there is little or no change in its polarity in going from the ground to excited state, as expected for this highly symmetric, nonpolar molecule.

In terms of its steady state spectroscopy, PP behaves in a straightforward manner. When we measured its fluorescence lifetime as a function of solvent, however, we find that the lifetime increased by more than a factor of 2 in lower refractive index solvents. The measured fluorescence decay rates and quantum yields for peropyrene and perylene are given in Table 1, along with the relevant solvent parameters. The fluorescence lifetime showed no correlation with standard measures of solvent polarity, which ruled out the role of a charge transfer state. The quantum yield is essentially independent of solvent, suggesting that the radiative decay rate controls the solvent-dependent fluorescence lifetime. It is well-known that the solvent index of refraction n controls the local density of electromagnetic modes around a molecule, which in turn affects the molecule's ability to radiate away its excited state energy. Most experimental and theoretical studies suggest that this local field effect leads to a factor of n^2 enhancement in the observed radiative rate of a planar molecule,[37−40] that is,

$$k_{rad}^{obs} = k_{fl}\phi_{fl} = n^2 k_{rad}^{0} \quad (1)$$

where k_{rad}^{0} is the intrinsic radiative rate of the molecule in a vacuum ($n = 1$). Thus a plot of k_{rad}^{obs} versus n^2 should yield a straight line where the value k_{rad}^{0} can be obtained by the line's y-intercept at $n = 1$. This plot is shown in Figure 2 for both PER and PP. Both data sets appear linear as a function of n^2, and the slope for perylene yields a reasonable value of $k_{rad}^{0} = 1.1 \times 10^8\ s^{-1}$. The slope obtained from the PP data, on the other hand, is much steeper and yields a negative value for k_{rad}^{0}. Clearly, some other factor, beyond the usual local field effect, is contributing to the solvent dependence of k_{rad}^{obs} for PP.

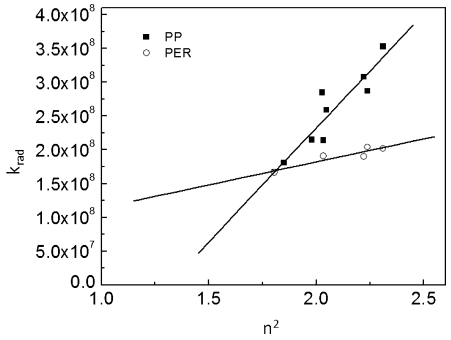

Figure 2. Rate of the radiative relaxation of monomeric peropyrene (black squares) and perylene (open circles) in different solvents plotted as a function of the solvent refractive index squared. The linear fits show that peropyrene has a negative y-intercept at $n^2 = 1$ while perylene has a positive y-intercept at n^2=1.

Table 1. Fluorescence Decay Rates and Quantum Yields for Peropyrene and Perylene

	solvent parameters[a]			$k_{fl}/10^8\ s^{-1}$[c]		φ_{fl}[d]	
solvent	ε_0	n	α	PP	PER	PP	PER
ACN	35.94	1.344	0.212	1.75	1.77	0.95	
ETOH	24.55	1.361	0.221	1.82		0.99	
THF	7.58	1.407	0.246	2.53		0.85	
DCM	8.93	1.424	0.255	3.16		0.90	
CH	2.02	1.426	0.256	2.38	2.03	0.90	0.94
DMF	36.71	1.431	0.259	2.88		0.90	
$CHCL_3$	4.89	1.446	0.289	3.62	2.02	0.85	
TOL	2.38	1.497	0.292	3.33	2.17	0.86	
CB	5.62	1.525	0.304	3.92	2.15	0.90[b]	

[a]Values obtained from ref 64. [b]Estimated value; average of all other measured PP quantum yield values. [c]Estimated error ±0.10. [d]Estimated error ±0.03.

The literature on the spectroscopy of polyenes provides an important clue as to the origin of the anomalous dependence of PP's k_{rad}^{obs} on solvent. In the polyenes, the emission originates from a weakly allowed ^1A_g state while the bright ^1B_u state dominates the absorption. The ^1A_g state to ground state transition is formally forbidden, but gains oscillator strength by mixing with the nearby optically allowed ^1B_u state.[41−43] The relative energies of these states, and thus their degree of mixing, change in different solvents. This solvent-dependence of the oscillator strength has been observed in at least one other type of molecule,[44] and Hudson and co-workers have developed a detailed theory for this phenomenon in the polyenes.[45] Following their approach, below we use perturbation theory to illustrate the main aspects of this phenomenon as applied to the case of PP. We consider a three-level system where ϕ_0 is the ground electronic state and there are two electronic excited states: ϕ_1 with energy ε_1 and ϕ_2 with energy ε_2. Furthermore, we assume all three states are normalized and orthogonal, and that ϕ_1 is the bright state and ϕ_2 is the dark state, that is,

dx.doi.org/10.1021/jp4051116 | J. Phys. Chem. C 2013, 117, 16802−16810

$$\langle \phi_0|\hat{\mu}|\phi_1\rangle \neq 0$$
$$\langle \phi_0|\hat{\mu}|\phi_2\rangle = 0 \quad (2a,b)$$

where $\hat{\mu}$ is the dipole moment operator. In this model, ϕ_1 corresponds to the ^1B_u state that is one-photon allowed due to its different symmetry from the ground state ϕ_0. ϕ_2 corresponds to the ^1A_g state, which shares the same symmetry as the ground state and thus is one-photon forbidden but two-photon allowed. If ϕ_1 and ϕ_2 are coupled through a generic operator $\hat{V}$, then first order perturbation theory gives the following expression for the perturbed bright state:

$$|\Psi_1^{(\text{mixed})}\rangle = |\phi_1\rangle + \frac{|\langle \phi_1|\hat{V}|\phi_2\rangle|^2}{\varepsilon_2 - \varepsilon_1}|\phi_2\rangle \quad (3)$$

The normalized version of $|\Psi_1^{(\text{mixed})}\rangle$ is defined to be $|\Psi_1\rangle$, and the radiative decay rate from this state will be proportional to its transition dipole moment squared as well as the local field factor n^2,

$$k_{\text{rad}}^{\text{obs}} \propto n^2 |\langle \phi_0|\hat{\mu}|\Psi_1\rangle|^2 \quad (4)$$

Note that here we take the local field factor to be n^2, rather than the factor of $(9n^2)/(n^2 + 2)^2$ assumed in ref 45. If we assume that the perturbation term is small, eq 4 can be written as

$$k_{\text{rad}}^{\text{obs}} \propto n^2 |\langle \phi_0|\hat{\mu}|\phi_1\rangle|^2 \left[1 - \frac{|\langle \phi_1|\hat{V}|\phi_2\rangle|^2}{|\varepsilon_2 - \varepsilon_1|^2}\right] \quad (5)$$

We see that $k_{\text{rad}}^{\text{obs}}$ now depends on both the local field factor n^2 and the energy separation between states ϕ_1 and ϕ_2. The energies of these states depends on their interaction with the solvent dielectric, and to first order these energies are given by

$$\varepsilon_1 = \varepsilon_1^0 + P_1\alpha$$
$$\varepsilon_2 = \varepsilon_2^0 + P_2\alpha \quad (6a,b)$$

where ε_1^0 is the energy of state 1 in vacuum, P_1 is the polarizability of state 1, and α is the polarizability of the solvent. From this analysis, eq 5 can be written in the form

$$\frac{k_{\text{rad}}^{\text{obs}}}{n^2} \propto k_{\text{rad}}^0 \left[1 - \frac{\Gamma^2}{(\Delta\varepsilon + \Delta P\alpha)^2}\right] \quad (7)$$

where

$$\Delta\varepsilon = \varepsilon_2 - \varepsilon_1$$
$$\Delta P = P_2 - P_1 \quad (8a,b)$$

We estimate the polarizability of the solvent from its refractive index n,

$$\alpha = \frac{n^2 - 1}{n^2 + 2} \quad (9)$$

A plot of $k_{\text{rad}}^{\text{obs}}/n^2$ versus the solvent polarizability α should lead to a Lorentzian type dependence on α. In Figure 3, we plot $k_{\text{rad}}^{\text{obs}}/n^2$ versus α for both PER and PP. As expected, the PER data is flat to within the experimental error, indicating that no significant state mixing exists. For PP, on the other hand, there is an obvious dependence on α, indicating that the second term in eq 7 cannot be neglected and there is a solvent-dependent mixing of two excited electronic states. In the polyenes, the $k_{\text{rad}}^{\text{obs}}$ of the low energy ^1A_g state increases due to mixing with the strongly allowed ^1B_u state.[43] In PP, we appear to have the opposite situation, where the strongly allowed ^1B_u state is the low energy state whose $k_{\text{rad}}^{\text{obs}}$ is decreased by the proximity of the dark state. A fit to the PP data using eq 7 yielded values $k_{\text{rad}}^0 = 4.2 \times 10^8 \text{s}^{-1}$, $\Gamma^2/\Delta\varepsilon^2 = 1.27$, and $\Delta P/\Delta\varepsilon = 1.31$. These values are reasonable when compared to values obtained for polyenes,[45] although the value for k_{rad}^0 is almost a factor of 4 higher than PER and may overestimate the intrinsic radiative rate.

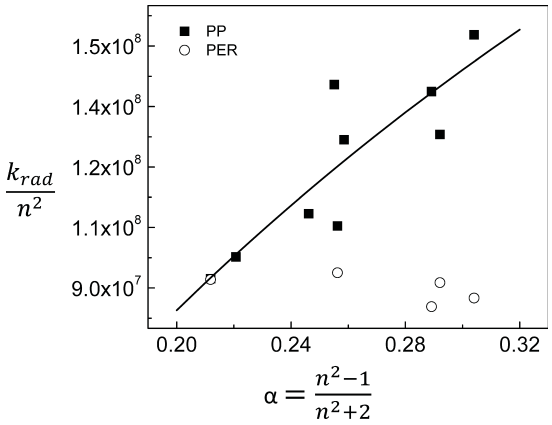

Figure 3. Rate of the radiative relaxation scaled by the solvent refractive index squared of PP (black squares) and PER (open circles) plotted as a function of the solvent property α, a function of the refractive index. Also shown is the fit of the PP data points (black curve) using eq 7 and the parameters given in the text. The PP rates change with α but those of PER do not.

To confirm that there is a dark state close in energy to the bright ^1B_u state, we measured the two-photon fluorescence excitation spectrum, which should reflect the shape of the $\phi_0 \rightarrow \phi_2$ transition. In Figure 4 we plot the two-photon fluorescence excitation spectra in two different solvents: acetonitrile (α = 0.219) and chlorobenzene (α = 0.304). Also shown are the one-photon absorption spectra for comparison. The one- and

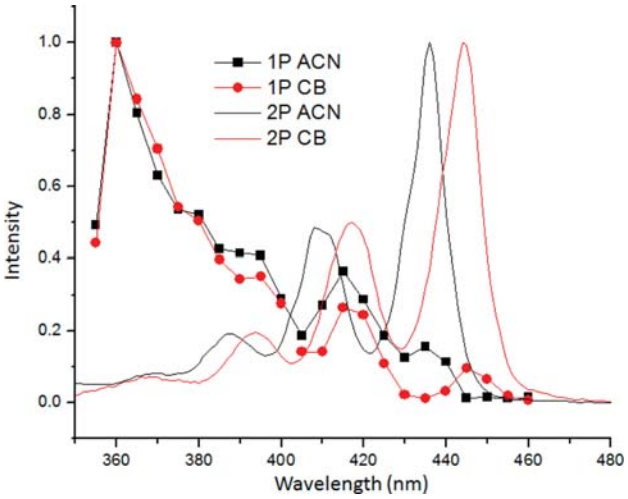

Figure 4. Normalized one-photon absorption (solid) and two-photon fluorescence excitation (symbols) spectra of PP in acetonitrile (ACN, black, n = 1.34) and chlorobenzene (CB, red, n = 1.52). The solvent-independent two-photon features at 395 and 415 nm are ascribed to the dark state, while the feature at ~440 nm that shifts with solvent is ascribed to residual two-photon absorption to the one-photon allowed state due to mixing with the dark state.

dx.doi.org/10.1021/jp4051116 | J. Phys. Chem. C 2013, 117, 16802−16810

two-photon lineshapes are completely different, indicating that the two different excitation modes access different states. A similar two-photon absorption line shape has been measured for PER,[46,47] and other workers have shown that PER derivatives have different one- and two-photon absorption spectra,[48,49] as expected for this class of highly symmetric molecules. In PP, the one- and two-photon spectra both exhibit similar vibronic progressions with spacings of ∼20 nm (corresponding to a 1000−1200 cm^{-1} vibrational mode characteristic of PAH's). Looking at the 415 nm peak in the two-photon spectra, we see that it does not shift with solvent, while the one-photon peak shifts from 437 to 450 nm. This shift moves the one-photon peak farther from the two-photon peak located at ∼415 nm. As the one-photon peak shifts farther away from the two-photon peak in higher α solvents, the degree of mixing should decrease and the k_{rad}^{obs} should increase, as observed experimentally. We suspect the two-photon peak around 440 nm reflects two-photon absorption to the bright $|\Psi_1\rangle$ state that is now two-photon allowed by virtue of the mixing between ϕ_1 and ϕ_2. The decrease in the amplitude of this peak as ϕ_1 shifts to lower energy in more polarizable solvents is consistent with a loss of its two-photon absorption strength which should accompany a decrease in mixing between ϕ_1 and ϕ_2. We do not think that the two-photon spectrum due to ϕ_2 is sensitive to the polarizability because the higher energy peaks at 395 and 415 nm do not shift with solvent.

The last question concerns the exact nature of the bright and dark states. We originally suspected that the dark state ϕ_2 might have ^1A_g symmetry, in analogy with the situation in the polyenes. As Schulten and Karplus originally showed,[50] this state can be thought of as a double excitation of two triplet states with overall singlet character. The existence of the T_1 state at almost exactly half the energy of the singlet S_1[27] would put this doubly excited state at the same energy as the singlet and approximately where the dark state is observed. Using time-dependent density functional theory (TDDFT) electronic structure calculations, we were able to assign ^1B_u symmetry to the bright state. The ground $^1A_g \rightarrow {}^1B_u$ transition is strongly dipole-allowed due to the change in state symmetry. Semi-empirical ZINDO and TDDFT calculations using B3LYP and wB97xd functionals all located a second singlet ^2B_u state at energies of 0.3−0.4 eV above the ^1B_u state, with an oscillator strength <1% of that of the bright ^1B_u state. The nearest ^1A_g state was at least 1 eV above the ^1B_u state, apparently ruling out any analogy with the polyenes. However, we are still left with some questions. If the dark state ϕ_2 we observe experimentally corresponds to the ^2B_u state, it is strange that its two-photon cross-section is so much larger than that of the ^1B_u state. In molecules of high symmetry, like PER and PP, two-photon absorption should couple states of like symmetry, for example, from a gerade ground state to a gerade excited state. Furthermore, standard ab initio methods often fail to correctly account for doubly excited electronic configurations,[51] and it is possible that a gerade singlet state is missed by our relatively simple calculations. The identity of the dark state merits further study.

To study PP in the solid-state, we grew single crystals from *o*-xylene and used X-ray diffraction to determine the crystal structure. The crystal parameters are summarized in Table 2, and two views of the crystal packing are shown in Figure 5. PP crystallizes in a herringbone pair motif, with an almost 90° angle between the π-stacked molecular pairs. The slight offset between the two molecules within the pair is commonly seen in the packing of similar PAH molecules.[52] The overall structure is very similar to that of α-perylene,[53] and this type of π-stacking is known to lead to strong electronic interactions and excimer formation.[54] The presence of such low energy states with charge-transfer character may provide a competing channel for relaxation of the initially excited singlet state and suppress SF.

Table 2. Crystal Data and Structure Refinement for Peropyrene

empirical formula	$C_{26}H_{14}$
formula weight	326.37
temperature	100(2) K
wavelength	0.71073 Å
crystal system	monoclinic
space group	$P2(1)/c$
unit cell dimensions	a = 12.377(3) Å, α = 90°
	b = 8.994(2) Å, β = 92.036(4)°
	c = 13.897(3) Å, γ = 90°
volume	1546.0(6) $Å^3$
Z	4
density (calculated)	1.402 mg/m^3
absorption coefficient	0.080 mm^{-1}
F(000)	680
crystal size	0.49 × 0.33 × 0.01 mm^3
theta range for data collection	1.65 to 25.68°
index ranges	$-15 \le h \le 15$, $-10 \le k \le 10$, $-16 \le l \le 16$
reflections collected	20 835
independent reflections	2926 [R(int) = 0.0852]
completeness to theta = 25.68°	100.00%
absorption correction	semiempirical from equivalents
max and min transmission	0.9989 and 0.9620
refinement method	full-matrix least-squares on F2
data/restraints/parameters	2926/0/235
goodness-of-fit on F2	1.005
final R indices [I > 2sigma(I)]	$R1$ = 0.0500, $wR2$ = 0.1246
R indices (all data)	$R1$ = 0.0948, $wR2$ = 0.1565
largest diff. peak and hole	0.240 and −0.211 e.$Å^{-3}$

To examine the effect of the crystal packing on the electronic dynamics, we measure the steady state and time-resolved spectroscopy of microcrystals of PP. Figure 6 shows the fluorescence emission spectra for a collection of PP micro-crystals at different temperatures. The spectra are red-shifted by ∼100 nm in the crystal relative to the solution spectrum in Figure 1a. Furthermore, the spectral shapes are quite different from those of the isolated molecule in solution; they are strongly broadened and the relative heights of the distinguishable peaks have changed. Some insight into the origin of these changes can be gained by examining the temperature dependence of the emission spectra. At lower temperatures, the peak at 550 nm becomes enhanced, while the shape of the emission at 650 nm and beyond remains constant. These separate changes suggest that at least two emitting species contribute to the total spectrum. The same situation is encountered for α−perylene, where the high and low energy emission components have been assigned to the Y- and E-type excimers, respectively.[53,55]

Time-resolved measurements confirm the presence of two distinct emitting species that appear to be created in parallel. In Figure 7, we show early (integrated from 0 to 1 ns) and late (integrated from 15 to 20 ns) luminescence spectra taken at

dx.doi.org/10.1021/jp4051116 | J. Phys. Chem. C 2013, 117, 16802−16810

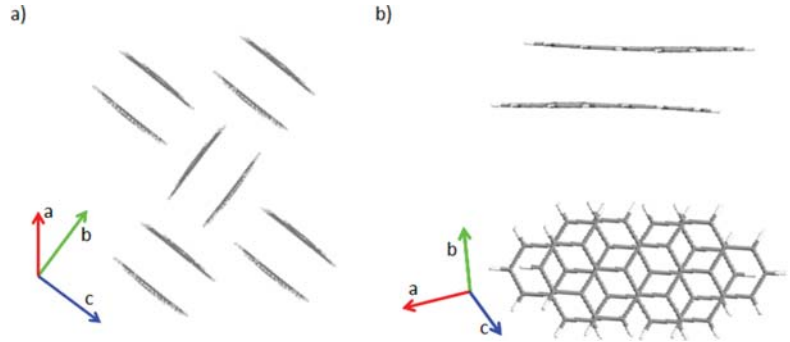

Figure 5. Two different views of crystalline PP: (a) side-view showing pairwise herringbone packing structur; (b) side and top view of each pair showing offset alignment of the PP molecular pair. The crystal unit cell axes are shown in both figures.

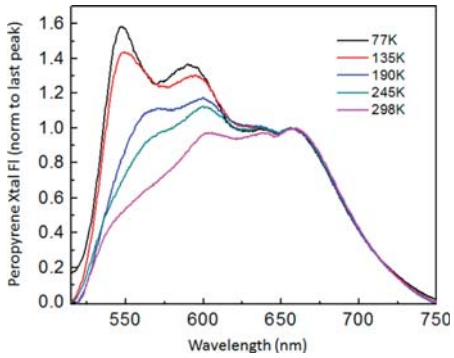

Figure 6. Normalized fluorescence emission spectra of crystalline PP at different temperatures. The higher energy peak at ~550 nm becomes more pronounced as the temperature is lowered.

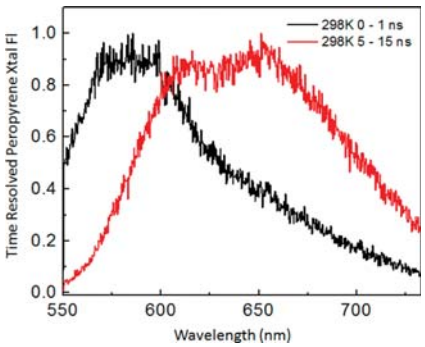

Figure 7. Normalized transient fluorescence spectra from crystalline PP at 298 K showing the early (integrated from 0 to 1 ns, black) emission spectral shape and the late emission (integrated from 5 to 20 ns, red). The time-dependent shift of the spectrum reflects the presence of two different species with different decay rates.

room temperature. The early time emission is dominated by the 550−600 nm emission, but this peak decays relatively quickly, leaving the longer time emission dominated by the double peaked spectrum (610 and 660 nm). The same qualitative shape change is also observed at 77 K, although at this temperature there is still appreciable 550−600 nm emission even in the long time window. The decay of the 550−600 nm peak depends on temperature, but that of the 610/660 nm feature is only weakly temperature dependent. This can be seen from the data in Figure 8a and b, which show the fluorescence decays centered at 550 and 650 nm, respectively. At both wavelengths, the decays are biexponential and can be fit using the parameters given in Table 3. It can be seen that the 550 nm peak decay time, τ_1, increases by a factor of 3.5 when the temperature is lowered to 77 K, while τ_2 doubles. The decay time of the 650 nm emission also lengthens at 77 K, but both components slow by less than a factor of 2. The nonexponential nature of the fluorescence decays could reflect disorder or a heterogeneous population of defects within the PP crystals. We found that the decay of the excimer in crystalline PER is sensitive to crystal quality. While solution-grown crystals had decay times on the order of 5 ns or less, and vacuum sublimed crystals had lifetimes on the order of 20 ns, decay times as long as 60−70 ns were observed in single crystals grown by sublimation of zone-refined material. We did not have sufficient sample to attempt this level of purification for PP. For this reason, we suspect that the τ_2 times in Table 3 represent a lower bound on the true fluorescence lifetime of crystalline PP.

There is no sign that the population in the high energy states is transferring into the 610/660 nm state, since if this were the case, we would expect to see the 610/660 nm component grow in on the τ_1 time scale. Neither signal exhibits a rise time, with both peaking within the 15 ps instrument response of the streak camera. Our data are consistent with an ultrafast relaxation of the initially excited state into two distinct emitting states that proceed to decay independently of each other. Again, this is very similar to the situation for α-perylene, where the excimer emission appears within 15 ps or less.[56−58] Earlier work suggested the E- and Y-states were formed independently from an initially excited "free exciton" population that rapidly partitions between high energy Y-state and a low energy E state in α-perylene.[55,59] Later temperature dependent measurements have suggested that there is population exchange between these states,[60] but the molecular origin of these two emitting species remains obscure. Nevertheless, we can conclude that the structural similarity between the PP crystals and α -perylene leads to a similarity of their spectroscopic properties as well.

The large changes in the electronic states of PP when it is in crystalline form have strong implications for its suitability as a SF material. It is doubtful that the triplet state experiences as large a shift as the singlet state in the crystal, and thus, the condition $E(S_1) \approx 2E(T_1)$ is likely no longer fulfilled. If we take the 550 nm peak to reflect the energy of the relaxed singlet, then $E(S_1)$=18 100 cm^{-1}, and if $E(T_1)$ =11 000 cm^{-1}, the SF reaction will be quite endothermic and not competitive with other relaxation processes. It is possible that there exists a short-lived higher energy state, analogous to the "free exciton" postulated for α-perylene, where SF is more favorable.

dx.doi.org/10.1021/jp4051116 | J. Phys. Chem. C 2013, 117, 16802−16810

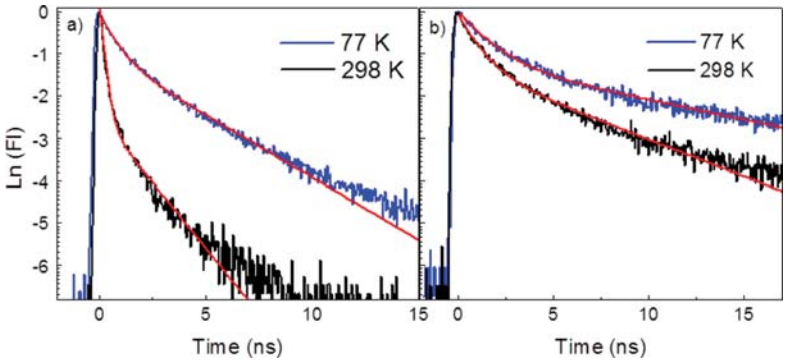

Figure 8. (a) The normalized fluorescence decays of crystalline PP at 298K (black) and 77K (blue) integrated over a 10 nm window centered at 550 nm. The corresponding biexponential fits (red, see Table 3 for formula and parameters) are also shown. (b) The same data as in panel (a), but integrated over a 10 nm window centered at 650 nm.

Table 3. Biexponential Decay Parameters Used to Fit the Fluorescence Decay Data in Figure 8

$f(t) = A_1 e^{-t/\tau_1} + A_2 e^{-t/\tau_2}$

	550 nm peak		650 nm peak	
parameter	77 K	298 K	77 K	298 K
A_1	0.61	0.92	0.69	0.70
τ_1 (ns)	0.701	0.198	1.477	0.978
A_2	0.39	0.08	0.31	0.30
τ_2 (ns)	3.389	1.617	10.755	5.732

However, the short lifetime (<15 ps) of such a state requires a rapid SF rate if it is going to generate a significant number of triplets. Our excitation wavelength of 400 nm (25 000 cm^{-1}) should provide sufficient excess energy to generate a pair of triplets, yet we saw no sign of delayed fluorescence that would indicate the creation of a large triplet population. Preliminary experiments also failed to observe a magnetic field effect on the fluorescence decay, which would also provide evidence for SF.[61,62] It is possible that triplets could be formed more efficiently from a higher-lying singlet state that is not accessed by our 400 nm excitation. Direct detection of triplets after variable wavelength excitation, for example using transient absorption with femtosecond time resolution, might provide some evidence for the existence of SF at very early times. But if SF can only occur from high-lying electronic states, its efficiency will be limited due to competition from internal conversion to the lowest-lying singlet state. While the lack of delayed fluorescence and a magnetic field effect does not conclusively prove that SF is completely absent, crystalline PP certainly does not behave like crystalline tetracene, a PAH with similar energetics where SF from the lowest singlet state plays a dominant role in the photophysics.

CONCLUSIONS

In this paper, we present a detailed investigation of the spectroscopy of PP, a PAH whose energy levels suggest that it could be a promising candidate for SF. In dilute solutions, PP's radiative rate shows an anomalous dependence on solvent polarizability that can be explained by mixing of the bright ^1B_u state with a higher energy dark state. We hoped that this dark state might be a precursor to a separated triplet pair state in the solid. However, the herringbone pair packing motif of the PP crystal appears to result in lower energy singlet excimer states that no longer satisfy the condition $2E(T_1) \leq E(S_1)$. This result suggests that control of the crystal packing could improve PP's potential as a SF material. For example, the β-form of perylene has a herringbone packing motif,[25,53] similar to that of tetracene, and apparently undergoes more facile SF.[24] If we can find conditions under which a similar crystal polymorph of PP is formed, we may be able to avoid excimer state formation and provide more time for SF to occur. Chemical substitution has also been shown to change the crystal packing of peropyrene derivatives,[63] providing a second way to crystal engineer a more promising SF material. Both approaches are currently being pursued, and in the future we hope to be able to more fully assess the potential of PP and related molecules as solid-state SF materials.

ASSOCIATED CONTENT

Supporting Information

^{1}H NMR spectrum of PP, UV−vis absorption spectrum of PP in toluene, and a Lippert-Matage plot of PP. This material is available free of charge via the Internet at http://pubs.acs.org.

AUTHOR INFORMATION

Corresponding Author

*E-mail: christopher.bardeen@ucr.edu.

Notes

The authors declare no competing financial interest.

ACKNOWLEDGMENTS

C.J.B. acknowledges support by the National Science Foundation under Grant CHE-1152677. V.M.N. and G.B.P. were supported by a Department of Education Graduate Assistance in Areas of National Need (GAANN). W.J.Y. acknowledges support from the University of North Texas in the form of startup funding and support by the National Science Foundation under Grant CHE-0840518.

REFERENCES

(1) Rieger, R.; Mullen, K. Forever Young: Polycyclic Aromatic Hydrocarbons as Model Cases for Structural and Optical Studies. *J. Phys. Org. Chem.* **2010**, *23*, 315−325.

(2) Paci, I.; Johnson, J. C.; Chen, X.; Rana, G.; Popovic, D.; David, D. E.; Nozik, A. J.; Ratner, M. A.; Michl, J. Singlet Fission for Dye-Sensitized Solar Cells: Can a Suitable Sensitizer Be Found? *J. Am. Chem. Soc.* **2006**, *128*, 16546−16553.

(3) Swenberg, C. E.; Geacintov, N. E. Excitonic Interactions in Organic Solids. In *Organic Molecular Photophysics*; Birks, J. B., Ed.; Wiley & Sons: Bristol, 1973; Vol. *1*, pp 489−564.

(4) Smith, M. B.; Michl, J. Singlet Fission. *Chem. Rev.* **2010**, *110*, 6891−6936.
(5) Ehrler, B.; Wilson, M. W. B.; Rao, A.; Friend, R. H.; Greenham, N. H. Singlet Exciton Fission-Sensitized Infrared Quantum Dot Solar Cells. *Nano Lett.* **2012**, *12*, 1053−1057.
(6) Jadhav, P. J.; Brown, P. R.; Thompson, N.; Wunsch, B.; Mohanty, A.; Yost, S. R.; Hontz, E.; Voorhis, T. V.; Bawendi, M. G.; Bulovic, V.; Baldo, M. A. Triplet Exciton Dissociation in Singlet Exciton Fission Photovoltaics. *Adv. Mater.* **2012**, *24*, 6169−6174.
(7) Congreve, D. N.; Lee, J.; Thompson, N. J.; Hontz, E.; Yost, S. R.; Reusswig, P. D.; Bahlke, M. E.; Reineke, S.; Voorhis, T. V.; Baldo, M. A. External Quantum Efficiency Above 100% in a Singlet-Exciton-Fission-Based Organic Photovoltaic Cell. *Science* **2013**, *340*, 334−337.
(8) Hanna, M. C.; Nozik, A. J. Solar Conversion Efficiency of Photovoltaic and Photoelectrolysis Cells with Carrier Multiplication Absorbers. *J. Appl. Phys.* **2006**, *100*, 074510/1−074510/8.
(9) Singh, S.; Jones, W. J.; Siebrand, W.; Stoicheff, B. P.; Schneider, W. G. Laser Generation of Excitons and Fluorescence in Anthracene Crystals. *J. Chem. Phys.* **1965**, *42*, 330−342.
(10) Burdett, J. J.; Muller, A. M.; Gosztola, D.; Bardeen, C. J. Excited State Dynamics in solid and Monomeric Tetracene: the Roles of Superradiance and Exciton Fission. *J. Chem. Phys.* **2010**, *133*, 144506/1−144506/12.
(11) Burdett, J. J.; Gosztola, D.; Bardeen, C. J. The Dependence of Singlet Exciton Relaxation on Excitation Density and Temperature in Polycrystalline Tetracene Thin Films: Kinetic Evidence for a Dark Intermediate State and Implications for Singlet Fission. *J. Chem. Phys.* **2011**, *135*, 214508/1−214508/10.
(12) Burdett, J. J.; Bardeen, C. J. Quantum Beats in Crystalline Tetracene Delayed Fluorescence Due to Triplet Pair Coherences Produced by Direct Singlet Fission. *J. Am. Chem. Soc.* **2012**, *134*, 8597−8607.
(13) Chan, W. L.; Ligges, M.; Zhu, X. Y. The Energy Barrier in Singlet Fission Can Be Overcome Through Coherent Coupling and Entropic Gain. *Nat. Chem.* **2012**, *4*, 840−845.
(14) Jundt, C.; Klein, G.; Sipp, B.; Moigne, J. L.; Joucla, M.; Villaeys, A. A. Exciton dynamics in pentacene thin films studied by pump-probe spectroscopy. *Chem. Phys. Lett.* **1995**, *241*, 84−88.
(15) Marciniak, H.; Pugliesi, I.; Nickel, B.; Lochbrunner, S. Ultrafast Singlet and Triplet Dynamics in Microcrystalline Pentacene Films. *Phys. Rev. B* **2009**, *79*, 235318/1−235318/8.
(16) Thorsmolle, V. K.; Averitt, R. D.; Demsar, J.; Smith, D. L.; Tretiak, S.; Martin, R. L.; Chi, X.; Crone, B. K.; Ramirez, A. P.; Taylor, A. J. Morphology Effectively Controls Singlet-Triplet Exciton Relaxation and Charge Transport in Organic Semiconductors. *Phys. Rev. Lett.* **2009**, *102*, 017401/1−017401/4.
(17) Rao, A.; Wilson, M. W. B.; Hodgkiss, J. M.; Albert-Seifried, S.; Bassler, H.; Friend, R. H. Exciton Fission and Charge Generation via Triplet Excitons in Pentacene/C60 bilayers. *J. Am. Chem. Soc.* **2010**, *132*, 12698−12703.
(18) Wilson, M. W. B.; Rao, A.; Clark, J.; Kumar, R. S. S.; Brida, D.; Cerullo, G.; Friend, R. H. Ultrafast Dynamics of Exciton Fission in Polycrystalline Pentacene. *J. Am. Chem. Soc.* **2011**, *133*, 11830−11833.
(19) Chan, W. L.; Ligges, M.; Jailaubekov, A.; Kaake, L.; Miaja-Avila, L.; Zhu, X. Y. Observing the Multiexciton State in Singlet Fission and Ensuing Ultrafast Multielectron Transfer. *Science* **2011**, *334*, 1541−1545.
(20) Ramanan, C.; Smeigh, A. L.; Anthony, J. E.; Marks, T. J.; Wasielewski, M. R. Competition Between Singlet Fission and Charge Separation in Solution-Processed Blend Films of 6,13-bis-(triisopropylsilylethynyl)pentacene with Sterically-Encumbered Perylene-3,4:9,10-bis(dicarboximide)s. *J. Am. Chem. Soc.* **2012**, *134*, 386−397.
(21) Wang, C.; Tauber, M. J. High-Yield Singlet Fission in a Zeaxanthin Aggregate Observed by Picosecond Resonance Raman Spectroscopy. *J. Am. Chem. Soc.* **2010**, *132*, 13988−13991.
(22) Johnson, J. C.; Nozik, A. J.; Michl, J. High Triplet Yield from Singlet Fission in a Thin Tilm of 1,3-diphenylisobenzofuran. *J. Am. Chem. Soc.* **2010**, *132*, 16302−16303.
(23) Ford, W. E.; Kamat, P. V. Photochemistry of 3,4,9,10-perylenetetracarboxylic Dianhydride Dyes. 3. Singlet and Triplet Excited-State Properties of the Bis(2,5-di-tert-butylphenyl)imide Derivative. *J. Phys. Chem.* **1987**, *91*, 6373−6380.
(24) Albrecht, W. G.; Coufal, H.; baberkorn, R.; Michel-Beyerle, M. E. Excitation Spectra of Exciton Fission in Organic Crystals. *Phys. Status Solidi B* **1978**, *89*, 261−265.
(25) Albrecht, W. G.; Michel-Beyerle, M. E.; Yakhot, V. Exciton Fission in Excimer Forming Crystal. Dynamics of an Excimer Build-Up in a-perylene. *Chem. Phys.* **1978**, *35*, 193−200.
(26) Takeda, Y.; Katoh, R.; Kobayashi, H.; Kotani, M. Fission and Fusion of Excitons in Perylene Crystal Studied with VUV and x-ray excitation. . *Electron Spectrosc. Relat. Phenom.* **1996**, *78*, 423−426.
(27) Wenzel, U.; Lohmannsroben, H. G. Photophysical and Fluorescence Quenching Properties of Peropyrene in Solution. *J. Photochem. Photobiol., A* **1996**, *96*, 13−18.
(28) Pogodin, S.; Agranat, I. Large PAHs by Reductive Peri-Peri "Dimerization" of Phenalenones. *Org. Lett.* **1999**, *1*, 1387−1390.
(29) Ueda, T.; Iwashima, S.; Aoki, J.; Takekawa, M. Complete Assignment and Additivity Rule for ^{1}H and ^{13}C Chemical Shifts of Non-Planar, Nonacyclic Aromatic Hydrocarbons. *Magn. Reson. Chem.* **1995**, *33*, 95−103.
(30) Dawson, W. R.; Windsor, M. W. Fluorescence Yields of Aromatic Compounds. *J. Phys. Chem.* **1968**, *72*, 3251−3260.
(31) Berlman, I. B. *Handbook of Fluorescence Spectra of Aromatic Molecules*; Academic Press: New York, 1971.
(32) Frisch, M. J.; Trucks, G. W.; Schlegel, H. B.; Scuseria, G. E.; Robb, M. A.; Cheeseman, J. R.; Scalmani, G.; Barone, V.; Mennucci, B.; Petersson, G. A.; et al. *Gaussian 09*, B.01; Gaussian Inc.: Wallingford, CT, 2009.
(33) Becke, A. D. Density-Functional Thermochemistry. 3. The Role of Exact Exchange. *J. Chem. Phys.* **1993**, *98*, 5648−5652.
(34) Schaefer, A.; Horn, H.; Ahlrichs, R. Fully Optimized Contracted Gaussian basis Sets For Atoms Li to Kr. *J. Chem. Phys.* **1992**, *97*, 2571−2577.
(35) Clar, E. *Polycyclic Hydrocarbons*; Academic Press: London, 1964.
(36) Fetzer, J. C.; Biggs, W. R. The High-Performance Liquid Chromatography of Peropyrene-Type Polycyclic Aromatic Hydrocarbons. *J. Chromatogr.* **1984**, *295*, 161−169.
(37) Shibuya, T. The Refractive-Index Correction to the Radiative Rate Constant. *Chem. Phys. Lett.* **1983**, *103*, 46−48.
(38) Lampert, R. A.; Meech, S. R.; Metcalfe, J.; Phillips, D.; Schaap, A. P. The Refractive Index Correction to the Radiative Rate Constant in Fluorescence Lifetime Measurements. *Chem. Phys. Lett.* **1983**, *94*, 137−140.
(39) Hirayama, S.; Iuchi, Y.; Tanaka, F.; Shobatake, K. Natural Radiative Lifetimes of Anthracene Derivatives and Their Dependence on Refractive Index. *Chem. Phys.* **1990**, *144*, 401−406.
(40) Toptygin, D. Effects of the Solvent Refractive Index and its Dispersion on the Radiative Decay Rate and Extinction Coefficient of a Fluorescent Solute. *J. Fluoresc.* **2003**, *13*, 201−219.
(41) Hudson, B. S.; Kohler, B. E. A low-lying weak transition in the polyene a,w-diphenyloctatetraene. *Chem. Phys. Lett.* **1972**, *14*, 299−304.
(42) Birks, J. B.; Tripathi, G. N. R.; Lumb, M. D. The Fluorescence of All-Trans Diphenyl Polyenes. *Chem. Phys.* **1978**, *33*, 185−194.
(43) Hudson, B. S.; Kohler, B. E.; Schulten, K. Linear Polyene Electronic Structure and Potential Surfaces. *Excited States* **1982**, *6*, 1−95.
(44) Mohanty, J.; Nau, W. M. Refractive Index Effects on the Oscillator Strength and Radiative Decay Rate of 2,3-diazabicyclo[2.2.2]oct-2-ene. *Photochem. Photobiol. Sci.* **2004**, *3*, 1026−1031.
(45) Andrews, J. R.; Hudson, B. S. Environmental Effects on Radiative Rate Constants with Applications to Linear Polyenes. *J. Chem. Phys.* **1978**, *68*, 4587−4593.
(46) Yu, J. A.; Nocera, D. G.; Leroi, G. E. Two-Photon Excitation Spectrum of Perylene in Solution. *Chem. Phys. Lett.* **1990**, *167*, 85−89.

(47) Vivas, M. G.; Diaz, C.; Echevarria, L.; Mendonca, C. R.; Hernandez, F. E.; Boni, L. D. Two-Photon Circular-Linear Dichroism of Perylene in Solution. *J. Phys. Chem. B* **2013**, *117*, 2742−2747.
(48) Belfield, K. D.; Bondar, M. V.; Hernandez, F. E.; Przhonska, O. V. Photophysical Characterization, Two-Photon Absorption and Optical Power Limiting of Two Fluorenylperylene Diimides. *J. Phys. Chem. C* **2008**, *112*, 5618−5622.
(49) Piovesan, E.; Silva, D. L.; Boni, L. D.; Guimaraes, F. E. G.; Misoguti, L.; Zalesny, R.; Bartkowiak, W.; Mendonca, C. R. Two-Photon Absorption of Perylene Derivatives: Interpreting the Spectral Structure. *Chem. Phys. Lett.* **2009**, *479*, 52−55.
(50) Schulten, K.; Karplus, M. On the Origin of a Low-Lying Forbidden Transition in Polyenes and Related Molecules. *Chem. Phys. Lett.* **1972**, *14*, 305−309.
(51) Dreuw, A.; Head-Gordon, M. Single-Reference *Ab Initio* Methods for the Calculation of Excited States of Large Molecules. *Chem. Rev.* **2005**, *105*, 4009−4037.
(52) Hunter, C. A.; Sanders, J. K. M. The Nature of π-π Interactions. *J. Am. Chem. Soc.* **1990**, *112*, 5525−5534.
(53) Tanaka, J. The Electronic Spectra of Aromatic Molecular Crystals. II. The Crystal Structure and Spectra of Perylene. *Bull. Chem. Soc. Jpn.* **1963**, *36*, 1237−1249.
(54) Birks, J. B. Excimers. *Rep. Prog. Phys.* **1975**, *38*, 903−974.
(55) Freydorf, E. V.; Kinder, J.; Michel-Beyerle, M. E. On Low Temperature Fluorescence of Perylene Crystals. *Chem. Phys.* **1978**, *27*, 199−209.
(56) Inoue, A.; Yoshihara, K.; Kasuya, T.; Nagakura, S. Excimer and Monomer Defect Emissions of Perylene and Pyrene Crystals as Studied by the Nanosecond Time-Resolved Spectroscopy Technique. *Bull. Chem. Soc. Jpn.* **1972**, *45*, 720−725.
(57) Kobayashi, T. The Observation of the Excimer Formation Process in Pyrene and Perylene Crystals Using a Picosecond Ruby Laser and Streak Camera. *J. Chem. Phys.* **1978**, *69*, 3570−3574.
(58) Nelson, K. A.; Dlott, D. D.; Fayer, M. D. Excited State Dynamics in Pure Molecular Crystals: Perylene and the Excimer Problem. *Chem. Phys. Lett.* **1979**, *64*, 88−93.
(59) Hochstrasser, R. M.; Nyi, C. A. Dynamical Effects from Resonance Raman and Fluorescence Studies of the Molecular Exciton System Perylene. *J. Chem. Phys.* **1980**, *72*, 2591−2600.
(60) Walker, B.; Port, H.; Wolf, H. C. The Two-Step Excimer Formation in Perylene Crystals. *Chem. Phys.* **1985**, *92*, 177−185.
(61) Geacintov, N.; Pope, M.; Vogel, F. Effect of Magnetic Field on the Fluorescence of Tetracene Crystals: Exciton Fission. *Phys. Rev. Lett.* **1969**, *22*, 593−596.
(62) Piland, G. B.; Burdett, J. J.; Kurunthu, D.; Bardeen, C. J. Magnetic Field Effects on Singlet Fission and Fluorescence Decay Dynamics in Amorphous Rubrene. *J. Phys. Chem. C* **2013**, *117*, 1224−1236.
(63) Beer, L.; Mandal, S. K.; Reed, R. W.; Oakley, R. T.; Tham, F. S.; Donnadieu, B.; Haddon, R. C. The First Electronically Stabilized Phenalenyl Radical: Effect of Substituents on Solution Chemistry and Solid-State Structure. *Cryst. Growth Des.* **2007**, *7*, 802−809.
(64) Reichardt, C. *Solvents and Solvent Effects in Organic Chemistry*; Wiley: Weinheim, Germany, 2003.